2-19-2018

Enhanced Light Extraction from OLEDs Fabricated on Patterned Plastic Substrates

Chamika M. Hippola
Iowa State University and Ames Laboratory, chamika@iastate.edu

Rajiv Kaudal
Iowa State University and Ames Laboratory, rkaudal@iastate.edu

Eeshita Manna
Iowa State University

Teng Xiao
Iowa State University and Ames Laboratory

Akshit Peer
Iowa State University and Ames Laboratory

See next page for additional authors

Enhanced Light Extraction from OLEDs Fabricated on Patterned Plastic Substrates

Abstract
A key scientific and technological challenge in organic light-emitting diodes (OLEDs) is enhancing the light outcoupling factor ηout, which is typically <20%. This paper reports experimental and modeling results of a promising approach to strongly increase ηout by fabricating OLEDs on novel flexible nanopatterned substrates that result in a >2× enhancement in green phosphorescent OLEDs (PhOLEDs) fabricated on corrugated polycarbonate (PC). The external quantum efficiency (EQE) reaches 50% (meaning ηout ≥50%); it increases 2.6x relative to a glass/ITO device and 2× relative to devices on glass/poly(3,4-ethylenedioxythiophene):polystyrene sulfonate (PEDOT:PSS) or flat PC/PEDOT:PSS. A significant enhancement is also observed for blue PhOLEDs with EQE 1.7× relative to flat PC. The corrugated PC substrates are fabricated efficiently and cost-effectively by direct room-temperature molding. These substrates successfully reduce photon losses due to trapping/waveguiding in the organic+anode layers and possibly substrate, and losses to plasmons at the metal cathode. Focused ion beam gauged the conformality of the OLEDs. Dome-shaped convex nanopatterns with height of ~280–400 nm and pitch ~750–800 nm were found to be optimal. Substrate design and layer thickness simulations, reported first for patterned devices, agree with the experimental results that present a promising method to mitigate photon loss paths in OLEDs.

Keywords
organic light-emitting diodes, outcoupling, phosphorescent OLEDs, plastic patterned substrates, solid state lighting

Disciplines
Materials Science and Engineering | Polymer and Organic Materials | Semiconductor and Optical Materials

Authors
Chamika M. Hippola; Rajiv Kaudal; Eeshita Manna; Teng Xiao; Akshit Peer; Rana Biswas; MicroContinuum, Inc.; Trovato Manufacturing, Inc.; Joseph Shinar; and Ruth Shinar

DOI: 10.1002/ ((please add manuscript number))
Article type: Full Paper

Enhanced Light Extraction from OLEDs Fabricated on Patterned Plastic Substrates

Chamika Hippola,[1,2§] Rajiv Kaudal,[1,2§] Eeshita Manna,[3] Teng Xiao,[1,2] Akshit Peer,[1,3,4] Rana Biswas,[1-4] W. Dennis Slafer,[5] Tom Trovato,[6] Joseph Shinar,[1,2] Ruth Shinar[3,4*]*

[1]Ames Laboratory, US Department of Energy, Iowa State University, Ames, IA 50011
[2]Physics & Astronomy Department, Iowa State University, Ames, IA 50011
Email jshinar@iastate.edu
[3]Electrical and Computer Engineering Department, Iowa State University, Ames, IA 50011
[4]Microelectronics Research Center, Iowa State University, Ames, IA 50011
Email rshinar@iastate.edu
[5]MicroContinuum, Inc., Cambridge, MA 02138
[6]Trovato Manufacturing, Inc., Victor, NY 14564
[§]These authors contributed equally to the paper

Keywords: OLEDs, plastic patterned substrates, outcoupling, solid state lighting

A key scientific and technological challenge in OLEDs is enhancing the light outcoupling factor η_{out}, which is typically <20%. We report experimental and modeling results of a promising approach to strongly increase η_{out} by fabricating OLEDs on novel flexible nano-patterned substrates that result in a >2x enhancement in green phosphorescent OLEDs (PhOLEDs) fabricated on corrugated polycarbonate (PC). The EQE reached 50% (meaning η_{out}>50%); it increased 2.6x relative to a glass/ITO device and 2x relative to devices on glass/PEDOT:PSS or flat PC/PEDOT:PSS. A significant enhancement was observed also for blue PhOLEDs with EQE 1.7x relative to flat PC. The corrugated PC substrates are fabricated efficiently by direct room-temperature molding in a cost-effective approach. These substrates successfully reduce photon losses due to trapping/waveguiding in the organic+anode layers and possibly substrate; losses to plasmons at the metal cathode are also reduced. Atomic force microscopy determined substrate morphology and anode current distribution. Focused ion beam gauged the conformality of the OLEDs. Dome-shaped convex nanopatterns with height of ~280-400 nm and pitch ~750-800 nm were optimal. Substrate design and layer thickness

simulations, reported first for patterned devices, agree with the experimental results that present a promising method to mitigate photon loss paths in OLEDs.

1. Introduction

OLEDs are widely used in displays, from smart phones to large TVs, as they provide thinner, brighter displays with vibrant colors and infinite contrast. They are also being developed for solid state lighting (SSL) applications. Unlike the bright point source emission of inorganic LEDs, OLEDs provide a cool or warm diffuse white source of light that is by default suitable for large area illumination. One of the primary criteria for OLEDs in SSL, together with cost reduction and increased stability, is improved light outcoupling (and hence efficiency), which remains a key scientific and technological challenge. The US Department of Energy (DOE) goal is an outcoupling factor (the ratio of the number of photons emitted into the "forward" hemisphere to the number of photons generated in the OLED) η_{out} = 70% by 2020, matching or exceeding that of current alternatives.

The external quantum efficiency *EQE* (the ratio of the number of photons emitted into the "forward" hemisphere to the number of electrons injected into the OLED) is given by[1,2]

$$EQE = \eta_{out}\, \gamma\, r_{ex}\, \Phi_{PL}, \quad [1]$$

and

$$\eta_{out} = EQE/IQE \quad [2]$$

where γ and Φ_{PL} are the charge balance factor and intrinsic photoluminescence (PL) quantum yield, respectively. r_{ex} is the radiative exciton recombination factor, which is ~0.25 for fluorescent materials, where only singlet excitons decay radiatively, but can approach 1 for phosphorescent materials, where both singlet and triplet excitons decay radiatively. *IQE* is the internal quantum efficiency, i.e., the ratio of the number of photons generated in the OLED to the number of electrons injected into it. It should be emphasized that while *EQE* can be measured directly, that is not the case for η_{out} or *IQE*, i.e., their determination is invariably model-dependent.[3-6] As $IQE \leq 1$, $\eta_{out} \geq EQE$. In some very specific cases (e.g., the green

phosphorescent OLEDs, PhOLEDs, described below) the parameters γ and Φ_{PL} can be adjusted to approach 1 by carefully choosing the materials and device architecture. Hence, almost 100% *IQE* is apparently achievable.[7-9]

The power efficiency of white PhOLEDs is already ~100 lm/W, comparable to that of LEDs and fluorescent tubes. This efficiency, however, is still far from the PhOLEDs' full potential with the main challenge being η_{out}.[2,10-12] The outcoupling is compromised by trapped or waveguided light loss inside the device and in the substrate due to refractive index mismatch, as well as losses to surface plasmons at the metal electrode.[2,10-12] Depending on the electron transport layer (ETL) thickness, up to 60% of the generated photons are lost mostly to (i) total internal reflection (TIR) at the glass/ITO interface (refractive indices n_{gl} ~ 1.5, n_{ITO} ~ 2.0) and subsequent waveguiding and loss in the organic+ITO layers ("internal waveguiding"), and (ii) surface plasmons at the metal cathode.[11,12] Another ~10% – 25% of the photons are trapped inside the glass substrate due to TIR at the glass/air interface and subsequent external waveguiding to the glass edges.[11-13] Thus, $\eta_{out} \leq 20\%$ with the conventional structure of through-the-glass-bottom-emitting-OLEDs.[11,12]

Extensive research has been performed in an attempt to improve η_{out} via different approaches. To extract the light lost in glass substrate modes, various sizes of microlens arrays (μLAs) were attached at the back of the glass,[13,14] TiO_2 nanoparticles[15] were embedded in the substrate, or high index substrates[16] replaced glass. A maximal 2x enhancement in the electroluminescence (EL) was achieved with a structured μLA when the μLA area exceeded that of the OLED pixel.[13]

Recovering the 40% – 60% light internally trapped in the organic+anode layers and/or lost to surface plasmons at the metal cathode remains particularly challenging. Use of high n ~1.7 polyimide (PI) with embedded air voids as scattering centers resulted in an η_{out} enhancement of 65% for green OLEDs; for white OLEDs (WOLEDs) *EQE* increased 1.6x from 11.9% to 19% and the power efficiency increased from 18 to 32 lm/W at 100 Cd/m^2.[17] The use of

colorless PI in a more complex procedure resulted in an increase of 1.9x in *EQE*, from 13.8% with glass/ITO to 26%.[18] Sub-anode designs with a non-diffractive dielectric scattering grid layer (e.g., SiO_2 with n ~1.5 or air grid in TiO_2, n ~2.2) between the transparent anode and the substrate were shown to enhance outcoupling of the internally waveguided light into the substrate.[19] An increase in *EQE* from ~15% to ~18% in a green PhOLED was reported. It increased to 40% with the addition of a μLA. The respective power efficiency increased from 36 to 43 to 95 lm/W with the μLA.[20] In a more complex design, a silver nanowire mesh in nano-imprinted polyethylene terephthalate (PET) substrate with a poly(3,4-ethylenedioxy-thiophene): polystyrene sulfonate (PEDOT:PSS) anode and an aperiodic nanostructure in the WOLED stack + μLA resulted in *EQE* = 46.3% (2.6x) at 1000 Cdm^{-2}.[21]

Another recent study focused on 1D grating, 2D grating, and quasirandom biomimetic nanostructures of PEDOT:PSS on flat PET/ITO where the highest EQE achieved was 12.5% (vs 8.3% for a flat device) for a green OLED.[22] Xiang et al.[23] employed a built-in Ag network electrode in patterned PET substrate, with the pattern apparently being on the "blank side." Hence, the enhancement due to this pattern is akin to a μLA used for extraction of substrate modes only.[13] Xu et al.[24] explored flexible transparent OLEDs with biomimetic nanostructured metal/dielectric composite electrode on a flat plastic. The pattern height was restricted to a single low value of h ~50 nm and a pseudo period 250 nm; conformality was not addressed. Chen et al.[25] described OLEDs fabricated on multilayer high conductivity/low conductivity PEDOT:PSS spin-coated on an ITO micromesh. However, the height of the ITO micromesh could only be roughly estimated at ~40 nm. The application of PEDOT:PSS reduced the corrugation height from 40 nm to 20 nm and the EQE was ~22%.

None of the foregoing studies explored the dependence of η_{out} on the substrate pattern height or pitch and only Chen et al.[25] evaluated the conformality of the OLED layers deposited on a micromesh ITO, though his structure required an external hemispherical lens

for enhancing the EQE above ~22%. Importantly, none evaluated the dependence of the OLED performance on the HTL or ETL thickness. In addition, none of these studies explored the separate roles of the nanopatterns in disrupting internal waveguiding *vs* disrupting surface plasmons.

Surface plasmon losses remain a major issue. A design of broad periodicity and random orientation in a buckling structure was shown to outcouple the surface plasmon mode in a green OLED.[26] A thicker *n*-doped ETL (with the doping needed to reduce the higher resistance associated with thicker layers) that increases the distance between the emitting layer and the metal cathode also weakens this loss channel.[11,12]

In this work enhanced light extraction exceeding 2x was achieved via fabrication of PhOLEDs with a PEDOT:PSS anode on flexible patterned polycarbonate (PC) substrates, with an effort to grow the OLED stack conformally on the patterned, scattering structure. Such structures disrupt the internal waveguiding in the organics+anode and reduce loss to surface plasmons at the metal cathode. The latter was achieved also with a thicker ETL that increases the distance between the emissive layer (EML) and the metal cathode. The PhOLEDs were broadly characterized via optoelectronic, structural, and chemical analyses. Flexible substrates of PET/CAB (cellulose acetate butyrate) were also studied.

Flexible substrates have many advantages over standard glass substrates. They are light weight, amenable to roll-to-roll (R2R) fabrication, cost effective, and have a relatively high refractive index $n_{PC} \approx 1.6$. Consequently they can play a crucial role in advancing OLED-based SSL and wearable devices of interest in medical and sensing applications.

Conductive ITO is extensively used as the anode in OLEDs because of its high transparency in the visible and preferred work function for hole injection into the organics.[27] However, its refractive index $n_{ITO} \sim 2$ is high and exacerbates the internal waveguiding losses. Unlike ITO, PEDOT:PSS ($n_{PEDOT:PSS} \sim 1.5$) does not present a refractive index mismatch with

the substrate,[28,29] resulting in more light extraction due to reduced internal waveguided losses in the organic+anode layers.[28]

Initially PEDOT:PSS was used only as a buffer layer between ITO and the organic layers due to its lower conductivity but efficient hole injecting properties.[30,31] However, it has become increasingly attractive as an anode with the commercial availability of high conductivity PEDOT:PSS and with conductivity-enhancing approaches obtained via mixing or treating with additives such as ethylene glycol (EG).[32-37] Cai et al.[28,34] showed that a spin-coated double layer PEDOT:PSS anode treated with EG yields superior anodes for green PhOLEDs in comparison to ITO. In future commercial devices however, an integrated substrate/anode with a metal mesh conductor and a thin ITO is envisioned.

2. Results and Discussion

2.1. Substrate Pattern and Anode

2.1.1. Characterization of nano-pattern substrates

All PC substrates had convex, dome-shaped nano-patterns (**Figure 1**) with the height *h* of the features ranging from 80 to 650 nm and a constant pitch *a* ~ 750 – 800 nm. Substrates based on PET/CAB with concave features had *h* ~220 - ~600 nm and *a* ~0.75 – 3 μm; the concave PET/CAB substrates were found to be inferior to the convex PCs. As mentioned, the nano-patterns on the substrates are expected to produce corrugation throughout the OLED stack, which should increase forward light extraction. This increased extraction is due to random changes in the incident angle at the organic+anode/substrate and possibly also substrate/air interfaces. The corrugation reduces also surface plasmon-related losses at the metal cathode.

The different plastic substrates were imaged via atomic force microscopy (AFM) for determining *h* and *a*. Figure 1 shows 3D AFM images of a nano-patterned PC substrate with *h* ~320 nm and *a* ~750 nm, and a PET/CAB/ITO with *h* ~250 nm and *a* ~1.75 μm.

2.1.2. Anode Fabrication

Figure 1 shows also a focused ion beam (FIB) image of an ITO section on a corrugated PET/CAB. As seen, there are some damaged areas, which may be due to stress induced in the thick (>100 nm) ITO deposited on the patterned substrates and/or damage to the corrugated surface occurring before or during ITO deposition. Chemical analysis of the damaged and intact areas revealed largely ITO and surface carbon in both areas. Importantly, due to a low CAB softening temperature (~70°C), the ITO was sputter-deposited at room temperature, which reduced its quality, as was also evident in its sheet resistance compared to that of glass/ITO deposited at ~220°C. Hence, to assess the feasibility of the patterned plastic substrates in enhancing light extraction, we resorted to a PEDOT:PSS anode while continuing to optimize the ITO anode in an integrated substrate/anode design for future lighting applications. While double layered PEDOT:PSS on a planar glass substrate serves as an excellent alternative anode to ITO on glass,[28] the wettability of the aqueous polymer solution on a plastic substrate is poor. As a result, the adhesion of the PEDOT:PSS film to plastic substrates is generally inadequate and leads to potential film delamination, which results in the well-known non-emissive dark spots.[38]

To reduce the surface tension of PEDOT:PSS at the interface with the hydrophobic plastic substrate, the polymer solution has to be treated with an additive. The wetting improves when the aqueous PEDOT:PSS solution is mixed with alcohols and/or fluorosurfactants.[39] Indeed, addition of 25% or 50% ethanol increases the wettability of PEDOT:PSS on PC, but reduces the conductivity significantly. The turn-on voltage of a standard NPB (*N,N′*-di(1-naphthyl)-*N,N′*-diphenyl-(1,1′-biphenyl)-4,4′-diamine)/Alq_3 (tris(8-hydroxyquinolinato)/CsF/Al OLED increased to 7.4 – 10.2 V *vs* 2.9 V for a similar OLED on glass/ITO. In contrast, addition of a fluorosurfactant, e.g., Zonyl FS30 or Capstone FS35, reduces the surface tension considerably without affecting the conductivity of the PEDOT:PSS film.[40] Some studies demonstrated an enhanced conductivity of PEDOT:PSS even upon adding a fluorosurfactant at a very low

concentration.[41] Here PEDOT:PSS was mixed with EG and 0.5% – 1% of Zonyl FS30 or Capstone FS35 fluorosurfactant. For a double layer PEDOT:PSS anode with each layer spin-coated at 3000 rpm for 30 s, a sheet resistance of ~170 Ohm/sq was achieved, which is slightly higher than the sheet resistance reported by Cai et al..[28] A double layered PEDOT:PSS film fabricated as described above[28] and in particular a single layer spin-coated at 6000 rpm proved to be optimal anodes for green and blue PhOLEDs, depending on the device structure.

Mapping the current distribution on the patterned double-layer PEDOT:PSS anode via conductive AFM (c-AFM) (**Figure S1**) demonstrated a non-uniform current distribution with, as expected, a higher current through the troughs and a lower current at the nano-pattern peaks. Thinner PEDOT:PSS showed a more uniform current distribution.

Figure S1 also shows the sheet resistance of PEDOT:PSS layers prepared at different spin rates and durations. While the resistance of a thin PEDOT:PSS anode is higher than that of the typical ~130 nm ITO, it proved important in demonstrating the promise of PhOLEDs on corrugated flexible substrates, as thicker solution-processed coatings were not uniform. They reduced the corrugation, i.e., filling more of the troughs, as indicated in **Table 1** (measurement by AFM). **Table S1** shows that the corrugation further decreased following device fabrication on PC-320 (i.e., PC with corrugation height *h* ~320 nm). *Importantly, the thin single layer PEDOT:PSS (~20-30 nm) spin coated at 6000 rpm for 30 s did not result in a change in the corrugation height within the ~8% experimental error, i.e., the PEDOT:PSS was deposited conformally.*

2.2. Evaluation of the conformal structure

To assess the conformality of the OLED stack we used FIB. A thick ITO layer (~130 nm) or a 2-layer PEDOT:PSS anode (~65 nm) resulted in a reduced corrugation of the OLED stack and Al cathode for green PhOLEDs on PC-320 (Table S1). In contrast, devices with the thin

single PEDOT:PSS layer on PC-320 or ITO on the PET/CAB did not show such a reduction as seen in **Figure 2**, though some thickness variations across the features were observed. The more conformal structure may be related to the solution-processed thinner anode on PC-320 and larger *a/h* ratio of the PET/CAB substrate.

The expected organic stack thickness of this specific device, based on the quartz crystal monitor in the evaporation chamber within the glovebox, is ~125 nm. The observed thickness was ~130 nm in the troughs and ~120 nm on the top of the corrugation, a difference of only ~8%. On the slopes we measured an average of ~100 nm, a reduction of ~23% in the thickness. The similarity of the thickness of the corrugated and flat layers is surprising due to the significantly larger surface area of the former but appears to be related to the a/*h* ratio that is high in this case. We note that for further development of this approach for future applications tilting and rotation of the substrate may be of benefit. Importantly, the corrugation height measured at the top Al layer was ~265 nm, similar to *h* ~250 nm measured for the bare substrate by AFM. The Al thickness was ~109 nm.

We next show results of enhanced outcoupling in patterned PhOLEDs using a PEDOT:PSS anode.

2.3. Green and Blue PhOLEDs

2.3.1. Green PhOLEDs – Design 1: Double layer PEDOT:PSS anode

To determine the optimal *h* for maximum light extraction, green tris (2-phenylpyridine) iridium(III) ($Ir(ppy)_3$)-based PhOLEDs with two different structures were evaluated. In one, the structure was:

PEDOT:PSS (two layers) anode / MoO_3 (1 nm)/10% MoO_3:NPB (22.5 nm) / NPB (22.5 nm)/ 6% $Ir(ppy)_3$:CBP (11 nm)/BPhen (40 nm) / LiF (1nm) / Al (100 nm).

Such structures were fabricated on different patterned PCs. The OLED layers were thermally evaporated on the spin-coated double layer PEDOT:PSS anode. Light extraction increased

with the corrugation height of the convex patterned PCs for heights ~250 ≤ *h* ≤ 400 nm as compared to a flat PC; a maximum luminous efficiency of ~127 Cd/A was achieved for such optimized devices (**Figure 3).** This efficiency is ~1.6x higher than that of the device on flat PC. *EQE* similarly increased ~1.6x from ~22% to 36%. The OLED efficiency was actually reduced for patterns with *h* ~215 and ~500 nm. Importantly, the angular dependence of the electroluminescence (EL) spectra for these green PhOLEDs deviates only slightly from Lambertian (Figure 3b) and no significant change in the normal emission spectrum was observed (Figure 3a).

As described later, the devices further improved significantly with a thick hole transport layer (HTL), which likely masked fine structural or other defects in the corrugated plastic substrates.

As seen in Figure 3, the peak luminous efficiency was the highest for the devices on PC-280 and PC-320 (i.e., *h* ~280 nm and 320 nm, respectively). **Table S2** summarizes the results. We note that the roll-off of the efficiency and the devices' degradation were fast as they were not encapsulated and the PC is relatively porous to water vapor and oxygen. Permeated oxygen, whose level increases for the corrugated substrates due to their larger surface area, quenches the phosphorescence,[38] hence, encapsulated devices would not only be much more stable, but would also exhibit higher efficiencies, as the phosphorescent quenching by O_2 will lessen. Additionally, as shown by FIB analysis, the OLED stack including the Al cathode exhibited a corrugated structure, though the height of the corrugation decreased as shown in Table S1. This situation is likely due to the non-uniform ~65 nm PEDOT:PSS layer (Table 1) and was observed also for thick (>100 nm) ITO on PC. For better enhancement the fidelity of the conformal structure needs to be highly controlled, as described next.

2.3.2. Green PhOLEDs – Design 2: Single PEDOT:PSS anode and thicker HTL & ETL.

A single layer PEDOT:PSS anode resulted in a more uniform current distribution and the most conformal OLED stack, however the sheet resistance increased up to 1.3 kOhm/sq. The increased resistance indicates that other means for enhanced conductivity are necessary. We fabricated devices on such a thin anode with the addition of a thin HAT-CN (dipyrazino[2,3-f:2',3'-h]quinoxaline-2,3,6,7,10,11-hexacarbonitrile) layer and a thicker HTL to minimize the effect of substrate structural or other defects. We also employed a thicker ETL that enhances the device performance by reducing surface plasmon excitation loss due to increased EML/ metal electrode distance.

The PhOLEDs structure was:

Substrate/Anode/HAT-CN (5 nm)/10% MoOx:TAPC (120 nm)/HAT-CN (5 nm)/TAPC (20 nm)/ 6% $Ir(ppy)_3$:mCP (20 nm)/TmPyPb (20 nm)/20% CsF:TmPyPb (40 nm)/LiF (1 nm)/Al (100 nm). Experiments with various levels of the CsF dopant indicated that 20% is suitable for n-doping TmPyPb (3,3′-[5′-[3-(3-pyridinyl) phenyl][1,1′:3′,1″-terphenyl]-3,3″-diyl]bispyridine), but not BPhen (4,7-diphenyl-1,10-phenanthroline) or TPBi (2,2′,2"-(1,3,5-benzinetriyl)-tris(1-phenyl-1-*H*-benzimidazole)) ETLs. The substrate/anode were either glass/ITO, glass/PEDOT:PSS, flat PC/PEDOT:PSS, or PC-410/PEDOT:PSS (PC-410 is of *h* ~410 nm, *a* ~800 nm). We note that the reported values of the HOMO and LUMO of HAT-CN (-7.5 and -4.4 eV, respectively) are very deep,[42] indicating deep electron trap and high hole barrier. As the HAT-CN layers are thin, however, a possible scenario for the experimentally observed very good hole transport properties of HAT-CN may be a change in the energetics due to electron trapping by some HAT-CN molecules, which should raise the HOMO and LUMO levels of the charged and adjacent molecules.

Figure 4 shows optical images of some devices and their optoelectronic properties are summarized in **Table 2**. As seen, the light emitted from the corrugated device shows some diffraction due to the pattern. In all cases the EL peaked at 512 nm with a slightly increased

shoulder at longer wavelengths for the device on glass/ITO. The luminous and power efficiencies were the largest for the device fabricated on PC-410/PEDOT:PSS. The maximal luminous efficiency for the latter was 164 CdA^{-1} at ~200 – 300 Cdm^{-2}, 1.9x the ~87 CdA^{-1} of the PhOLED on glass/PEDOT:PSS, 2.4x the 67 CdA^{-1} of the device on glass/ITO, and 2x the 82 CdA^{-1} of a device on flat PC. The respective maximal power efficiencies for the four substrate/anode combinations were 150, 80, 70, and 70 lmW^{-1}, i.e., the enhancements were 1.9x and 2.1x. *The maximal EQE was 50% with enhancements of 2x relative to the device on glass/PEDOT:PSS and 2.6x relative to that on glass/ITO*. These enhancements are beyond those observed for the PhOLEDs with the thinner HTL and ETL. This is likely due to improved hole injection, masking of substrate non-uniformity and defect issues, and further enhanced outcoupling of photons otherwise lost to surface plasmon excitation.

As seen in Table 2, the highest *EQE* of 50% was obtained for a green PhOLED on PC-410, a 2x enhancement in comparison to such devices on glass and flat PC. This *EQE* entails $\eta_{out} \geq$ 50% (Equation 1). Significant enhancements were obtained also for the blue PhOLEDs. This situation may indicate that the enhancement is due mostly to extraction of photons trapped in the high index layers, as only small perturbations in the flat layer near the metal cathode are believed to be sufficient for disrupting surface plasmon excitation.

2.3.3. Blue PhOLEDs Design 2: Single layer PEDOT:PSS anode and thicker HTL & ETL

We note that the conformal fabrication of blue PhOLEDs with Design 1, i.e., a relatively thick two-layer PEDOT:PSS anode was challenging, though high enhancement were achieved as summarized in Table S2. Hence, we present here only devices with Design 2. The device structure was that of the green PhOLED, except that the emitting layer was 20 nm of 8% FIrpic:mCP. We note that it is likely that the optimal thickness of the various device layers (that will enhance the efficiencies) in green and blue PhOLEDs differ;[12] a determination of such thicknesses requires future detailed evaluation of various combinatorial arrays.

The device attributes are shown in **Figure 5**. The maximal luminous efficiency increased 2x from ~31 CdA^{-1} to ~62 CdA^{-1} at the patterned substrate. At ~1000 Cdm^{-2} the enhancement was ~1.8x, increasing from 30 CdA^{-1} on the flat PC to ~55 CdA^{-1} on the pattern. The maximal power efficiency increased from 16.9 lmW^{-1} to ~50 lmW^{-1}; a 3 fold enhancement; at ~700 Cdm^{-2} the enhancement was 1.7x; this reduction is due to a rapid roll off for the non-encapsulated corrugated device. Note that the roll off in the power efficiency is significantly steeper than in the luminous efficiency or *EQE*. This is direct proof that the resistance, probably that of the anode, is a major contributor to the power efficiency roll off. The maximal *EQE* increased to 25% from 15% for the flat device, a 1.7x enhancement. At ~1000 Cdm^{-2} the enhancement was 1.5 fold.

2.4. Computational modeling of the OLEDs

It is of great interest to predict the limits to outcoupling achievable in OLEDs using rigorous electromagnetic simulations to predict the optimum range of structures. Accordingly, we have employed two complementary computational approaches consisting of (i) Fourier space scattering matrix and (ii) real space finite difference time domain (FDTD) methods (see SI).

Scattering matrix simulations in Fourier space

The rigorous scattering matrix approach in Fourier space provides a quantitative estimate of η_{out} and power losses within the OLED. Several studies[11,12,43,44] have developed this approach for flat OLEDs to quantify the waveguided modes within the substrate and high-index layers, in addition to the plasmonic losses.

The corrugated OLEDs we fabricated pose a problem of considerable complexity, and the theory of light emission from such systems has *not* previously been developed. Accordingly, we have developed a rigorous scattering matrix based theory of light emission in corrugated

systems (to be published), based on the formalism developed for flat OLEDs.[11,12] Our theory includes:

a) A corrugated OLED where each layer is described by periodic dielectric functions $\varepsilon(r)$ and its Fourier components $\varepsilon(G)$, where G is a vector of the reciprocal 2-dimensional periodic lattice.

b) Dipoles in a conformally corrugated emissive layer forming annular rings at different heights z in the OLED. At each height the dipoles are described by a Fourier transform $H(G)$.

c) Light emission from the dipoles in a conformally corrugated emissive layer that are reflected from the cathode and the air-substrate interface to generate a reflected electric field $\mathbf{E}(u,G)$ in the emissive layer. Here u is the parallel component of the wavevector in the emissive layer.

d) The ability of the corrugated layers to scatter waveguided modes within the substrate and high index layer to the air through diffraction.

e) The Purcell factor of the emission rate, which is a lateral function of the planar coordinates x and y in each layer. This is converted into a Fourier transform of the convolution of the internal fields $E(u,G)$, and the dipole positions $H(G)$ and summed over all Fourier components G in the structure.

f) Independently summing the emission from 3 polarizations of the dipoles (transverse magnetic vertical (*TMv*), transverse magnetic horizontal (*TMh*), transverse electric horizontal (*TEh*); i.e. z, x, y) to obtain the emission rates of dipoles in the corrugated layer $K(TMv)$, $K(TMh)$, $K(TEh)$.

g) The emission of waves into the air region is simulated and modulated by the emission rates of dipoles in the corrugated layer for each of the three polarizations.

h) A summation of emission from each independent parallel component u of the wave-vector for the power emitted inside P_{in} and outside the structure P_{out}.

i) The outcoupling factor η_{out}, which is the ratio of the power emitted into the air to the total emission P_{out}/P_{in} at each wavelength.

Maxwell's equations are solved in Fourier space for the substrate/anode/HTL/ETL/Al cathode OLED with the emissive dipoles residing between the HTL and ETL. By computing the reflected modes from the air/substrate interface and the ETL/metal cathode interface, we obtain the fields at the location of the dipole emitter and the Purcell factor, which represents inhibition or enhancement of the emission rates due to the OLED optical cavity geometry.[11,12,43,44]

For a flat OLED with a PC or glass substrate, we simulated the outcoupling of light as a function of the ETL thickness, shown for a green OLED in **Figure 6**. There are two maxima in the outcoupled power, corresponding to ETL thicknesses of $\lambda/4$ (total optical thickness of $3\lambda/4$), and a second peak at an ETL thickness of $3\lambda/4$ (total optical thickness of $5\lambda/4$), in agreement with previous reports.[11,12] Only <15% of the light is emitted to air within the first maximum.

The outcoupling was computed as a function of the thickness of the ETL (d ETL) layer. Initial results suggest a weak dependence on the ETL layer thickness. Numerically ill-converged regions around u ~1.0 were truncated. We obtain η_{out} *reaching 60%* for both 200 nm and 300 nm corrugation heights, for a range of ETL thicknesses including an ETL layer thickness of ~85 nm at 200 nm corrugation height. We utilized a PC substrate with n = 1.56 in the green OLED (λ = 510 nm) similar to the experiment. We utilized the annular ring with the largest density of dipole emitters located closest to the air-polycarbonate interface. The outcoupling dramatically exceeds that of a flat glass/ITO OLED where the outcoupling was <15%. Further studies will optimize the structure to maximize the outcoupling.

3. Summary and Concluding Remarks

We demonstrated outcoupling enhancements of 1.5- to ~3-fold using various nano-corrugated PC substrates for green and blue PhOLEDs with a PEDOT:PSS anode. The enhancements depend on the structure and height of the corrugation, and the PEDOT:PSS thickness has an effect on the device conformality and hence performance. The largest enhancement was achieved for devices fabricated on convex patterns with a corrugation height *h* ~280-400 nm and pitch of ~750-800 nm. The observed enhancements are due to the effect of the corrugation on the extraction of the internally waveguided light and also on reducing loss to surface plasmon excitation at the Al metal cathode.

The anode thickness was optimized to achieve a more conformal OLED stack and thus a more uniform current distribution. While an integrated substrate/anode with a metal mesh conductor, to reduce the resistance, and a thin ITO layer will further improve the devices, currently the best devices were achieved with a thin PEDOT:PSS (~20 - 30 nm) anode. A thermally evaporated ITO can replace the PEDOT:PSS anode and conformal structures were observed using FIB, but ITO's high $n \sim 2$ is problematic and fabricating a high quality ITO typically requires elevated temperatures, which is an issue with most plastic substrates. Surprisingly, the layers' thickness on the corrugated substrates were similar to those on flat substrates despite the larger surface area.

Importantly, devices with doped thick HTL and ETL demonstrated improved performance. The thick HTL provided a cover to some of the substrates' defects that can otherwise lead to shorts. The thick ETL increased the distance between the cathode and the emissive layer, hence reducing plasmon excitation loss. Doping of the thicker layers was necessary for reducing the resistance of the devices. Device encapsulation, in particular a barrier layer integrated with the substrate/anode to prevent moisture and O_2 from penetrating the relatively porous plastic, will lead to high efficiencies at high brightness and minimize quenching of the phosphorescence by O_2.

The simulations, reported for the first time for patterned devices, and experiment generally agree that large corrugation heights of ~200-400 nm are necessary to achieve enhanced light outcoupling from OLEDs. The simulations suggest also that corrugations can reduce plasmonic losses that are particularly severe in thin flat OLEDs. The simulated outcoupling of η_{out} ~60% is consistent with the measured maximal *EQE* of 50% for green corrugated PhOLEDs on PC/PEDOT:PSS. Improving the conformality of the devices is ongoing, including utilizing predictive simulations to achieve a guiding maximal enhancement.

4. Experimental

Materials: The flat and patterned PC and PET/CAB substrates with various pattern heights and pitches were fabricated by MicroContinuum, Inc. The conductive polymer PEDOT:PSS, used as the anode, was purchased from H. C. Starck. LiF, BPhen, FIrpic, and the yellow emitter rubrene were purchased from Sigma-Aldrich. MoO_3 was purchased from Sterm Chemicals, and NPB-and Alq_3 from HW Sands Corporation. HAT-CN, TAPC, CBP, 3TPYMB, TmPyPB, and $Ir(ppy)_3$ were purchased from Luminescence Technology Corporation.

Corrugated PC and PET/CAB fabrication: The patterned substrates were fabricated by proprietary processes developed by MicroContinuum Inc. (www.microcontinuum.com). The corrugated PC is fabricated by an efficient, direct near room-temperature molding process so that there is no patterned layer/substrate interface, which eliminates peel off and index mismatch losses. The process eliminates thermal distortion and/or degradation and reduces production time by avoiding slow heating/cooling cycles required by conventional thermal molding processes. A single template with constant pitch was used to produce a wide range of

amplitudes of the features' height without the cost/time required for fabricating new templates for each amplitude to be studied.

The corrugated PET/CAB substrates are generated by using the above process on a 12 µm thick layer of CAB previously slot coated onto a 75 µm thick PET carrier substrate. This approach enables independent optimization of the physical and optical characteristics of the patterned layer and the carrier substrate, including adjustment of the refractive index by modifying the patterned layer and the tear resistance of the carrier layer.[45-47]

PEDOT:PSS film fabrication and characterization: The PEDOT:PSS solution was mixed with 6 v% EG and 1 v% Capstone FS35 fluorosurfactant. The mixed solution was filtered using a 0.45 µm syringe filter. The solution was spun at various spin rates and spin durations. For example, a single layer of PEDOT:PSS was deposited by spin coating the mixed solution at 6000 rpm for 30 s followed by annealing the film on a hot plate at 120^{o}C for 5 min. The second PEDOT:PSS layer was formed following the same procedure. The resulting film was annealed at 120^{o}C for 1 h in air and for 1 h in the glovebox. Sheet resistances were measured using a four point probe setup with a source measurement unit (Keithley 200 and Fluke 8842A). The morphology of the films was obtained by AFM (TESPA) employing tapping mode; current distribution maps were imaged by conductive AFM employing contact mode.

FIB Imaging: For analysis of the OLED structure and stack conformality we used a FEI Helios DualBeam FIB/SEM system that combines sputtering, imaging, and analytical capabilities. The system enables very precise ion milling in selected areas as well as high-resolution 3-D microscopy. A beam of gallium ions is used for nm precision milling and imaging, depending on the ion energy and intensity; the Ga^{+} ion source can image and machine down to 5 nm resolution levels. The system enables also chemical analysis using x-ray EDS (energy dispersive spectroscopy).

OLED fabrication and characterization: OLEDs were fabricated on the PEDOT:PSS-coated corrugated and flat plastic substrates as well as on glass/ITO and glass/PEDOT:PSS substrates for reference. The Al cathode and all organic materials were deposited by thermal evaporation inside a chamber with a base pressure of $\sim 10^{-6}$ mbar within a glovebox. The Al cathode was deposited through a shadow mask containing either 1.5 mm diameter circular holes or 3 mm wide stripes. Characterization of the OLEDs was done using a Keithley 2400 source meter to apply a voltage and measure the current. The brightness was measured by a Minolta LS110 luminance meter and the EL spectra were obtained using an Ocean Optics PC2000-ISA spectrometer. The raw spectra were obtained in the "SCOPE" mode, but were corrected to the radiometrically calibrated mode; the spectra shown are the corrected spectra. Labview software was used to calculate the efficiencies from the experimental data.

Supporting Information
Supporting Information is available from the Wiley Online Library or from the author.

Acknowledgements
The work was supported by DOE/EERE Grants DE-SC0011337 and DE-EE0007621. Ames Laboratory is operated by Iowa State University for the USDOE under Contract No. DE-AC 02-07CH11358. The research was partially supported by Basic Energy Sciences, Division of Materials Science and Engineering, USDOE.

Received: ((will be filled in by the editorial staff))
Revised: ((will be filled in by the editorial staff))
Published online: ((will be filled in by the editorial staff))

References

[1] J. Shinar, V. Savvateev, in *Organic Light-Emitting Devices: A Survey* (Ed.: J. Shinar), Springer, New York, **2004**, chapter 1, pp. 1 – 41.

[2] J.-S. Kim, P. K. H. Ho, N. C. Greenham, R. H. Friend, *J. Appl.Phys.* **2000**, *88*, 1073.

[3] X.-W. Chen, W. C. H. Choy, C. J. Liang, P. K. A. Wai, S. He, Appl. Phys. Lett. **2007**, *91*, 221112.

[4] M. Flämmich, N. Danz, D. Michaelis, C. A. Wächter, A. H. Bräuer, M. C. Gather, K. Meerholz, in *Light-Emitting Diodes: Materials, Devices, and Applications for Solid State Lighting XIV* (Eds: Klaus P. Streubel, Heonsu Jeon, Li-Wei Tu, Norbert Linder), *Proc. SPIE* **2010**, *7617*, 761715.

[5] M. Furno, T. C. Rosenow, M. C. Gather, B. Lüssem, K. Leo, *Appl. Phys. Lett.* **2012**, *101*, 143304.

[6] T. Miwa, S. Kubo, K. Shizu, T. Komino, C. Adachi, H. Kaji, *Sci. Repts.* **2017**, *7*, 284.

[7] M. A. Baldo, D. F. O'Brien, Y. You, A. Shoustikov, S. Sibley, M. E. Thompson, S. R. Forrest, *Nature* **1998**, *395*, 151.

[8] M. A. Baldo, S. Lamansky, P. E. Burrows, M. E. Thompson, S. R. Forrest, *Appl. Phys. Lett.* **1999**, *75*, 4.

[9] T. Tsutsui, M.-J. Yang, M. Yahiro, K. Nakamura, T. Watanabe, T. Tsuji, Y. Fukuda, T. Wakimoto, S. Miyaguchi, *Jpn. J. Appl. Phys.* **1999**, *38*, L1502.

[10] C. F. Madigan, M.-H. Lu, J. C. Sturm, *Appl. Phys. Lett.* **2000**, *76*, 1650.

[11] R. Meerheim, M. Furno, S. Hofmann, B. Lüssem, K. Leo, *Appl. Phys. Lett.* **2010**, *97*, 253305.

[12] M. Furno, R. Meerheim, S. Hofmann, B. Lüssem, K. Leo, *Phys. Rev. B* **2012**, *85*, 115205.

[13] J.-M. Park, Z. Gan, W. Y. Leung, Z. Ye, K. Constant, J. Shinar, R. Shinar, K.-M. Ho, *Opt. Exp.* **2011**, *19*, A786.

[14] S. Möller, S. R. Forrest, *J Appl. Phys.* **2002**, *91*, 3324

[15] C.-H. Chang, K.-Y. Chang, Y.-J. Lo, S.-J. Chang, H.-H. Chang, *Org. Electr.* **2012**, *13*, 1073.

[16] G. Gaertner, H. Greiner, *Proc. SPIE Organic Optoelectronics and Photonics III*, **2008**, *6999*, 69992T.

[17] T.-W. Koh, J. A. Spechler, K. M. Lee, C. B. Arnold, B. P. Rand, *ACS Phot.* **2015**, *2*, 1366.

[18] J. A. Spechler, T.-W. Koh, J. T. Herb, B. P. Rand, C. B. Arnold, *Adv. Func. Mater.* **2015**, *25*, 7428.

[19] Y. Sun, S. R. Forrest, *Nat. Phot.* **2008**, *2*, 483.

[20] Y. Qu, M. Slootsky, S. R. Forrest, *Nat. Phot.* **2015**, *9*, 758.

[21] L. Zhou, H.-Y. Xiang, S. Shen, Y.-Q. Li, J.-D. Chen, H.-J. Xie, I. A. Goldthorpe, L.-S. Chen, S.-T. Lee, J.-X. Tang, *ACS Nano* **2014**, *8*, 12796.

[22] R. Wang, L.-H. Xu, Y.-Q. Li, L. Zhou, C. Li, Q.-D. Ou, J.-D. Chen, S. Shen, and J.-X. Tang, *Adv. Opt. Mater.* **2015**, *3*, 203.

[23] H.-Y. Xiang, Y.-Q. Li, L. Zhou, H.-J. Xie, C. Li, Q.-D. Ou, L.-S. Chen, C.-S. Lee, S.-T. Lee, and J.-X. Tang, *ACS Nano* **2015**, *9*, 7553.

[24] L.-H. Xu, Q.-D. Ou, Y.-Q. Li, Y.-B. Zhang, X.-D. Zhao, H.-Y. Xiang, J.-D. Chen, L. Zhou, S.-T. Lee, and J.-X. Tang, *ACS Nano* **2016**, *10*, 1625.

[25] C.-Y. Chen, Y.-J. Chen, W.-K. Lee, C.-Y. Lu, H. Y. Lin, and C.-C. Wu, *Opt. Express* **2016**, *24*, A810-A822.

[26] W. H. Koo, S. M. Jeong, S. Nishimura, F. Araoka, K. Ishikawa, T. Toyooka, H. Takezoe, *Adv. Mater.* **2011**, *23*, 1003.

[27] F. Nuesch, E. W. Forsythe, Q. T. Le, Y. Gao, L. J. Rothberg, *J. Appl. Phys.* **2000**, *87*, 7973.

[28] M. Cai, Z. Ye, T. Xiao, R. Liu, Y. Chen, R. W. Mayer, R. Biswas, K-M Ho, R. Shinar, J. Shinar, *Adv. Mater.* **2012**, *24*, 4337.

[29] J. Gasiorowski, R. Menon, K. Hingerl, M. Dachev, N. S. Sariciftci, *Thin Sol. Films* **2013**, *536*, 211.

[30] M. Cai, T. Xiao, E. Hellerich, Y. Chen, R. Shinar, J. Shinar, *Adv. Mater.* **2011**, *23*, 3590.

[31] T. Xiao, W. Cui, J. Anderegg, J. Shinar, R. Shinar, *Org. Electr.* **2011**, *12*, 257.

[32] J. Ouyang, Q. F. Xu, C. W. Chu, Y. Yang, G. Li, J. Shinar, *Polymer* **2004**, *45*, 8443.

[33] Y. H. Kim, C. Sachse, M. L. Machala, C. May, L. Muller-Meskamp, K. Leo, *Adv. Funct. Mater.* **2011**, *21*, 1076.

[34] M. Cai, T. Xiao, R. Liu, Y. Chen, R. Shinar, J. Shinar, *Appl. Phys. Lett.* **2011**, *99*, 153303.

[35] K. Fehse, K. Walzer, K. Leo, W. Lovenich, A. Elschner, *Adv. Mater.* **2007**, *19*, 441.

[36] S. I. Na, S. S. Kim, J. Jo, D. Y. Kim, *Adv. Mater.* **2008**, *20*, 4061.

[37] D. S. Hecht, L. B. Hu, G. Irvin, *Adv. Mater.* **2011**, *23*, 1482.

[38] J. Shinar, R. Shinar, *J. Phys. D: Appl. Phys.* **2008**, *41*, 133001.

[39] E. Hrehorova, M. Rebros, A. Pekarovicova, P.D. Fleming, V.N. Bliznyuk, *TAGA Journal* **2008**, *4*, 219.

[40] M. Vosgueritchian, D. J. Lipomi, Z. Bao, *Adv. Funct. Mater.* **2012**, *22*, 421.

[41] C. M. Palumbiny, J. Schlipf, A. Hexemer, C. Wang, P. Müller-Buschbaum, *Adv. Electron. Mater.* **2016**, *2*, 1500377.

[42] Y. Dai, H. Zhang, Z. Zhang, Y. Liu, J. Chena, D. Ma, *J. Mater. Chem. C* **2015**, *3*, 6809.

[43] K. G. Sullivan, D. G. Hall, *J. Opt. Soc. Am. B* **1997**, *14*, 1149.

[44 K. A. Neyts, *J. Opt. Soc. Am. A* **1998**, *15***,** 962.

[45] W. D. Slafer, M. B. Kime, M. J. Monen, W. G. Horton, W. C. Robinson, L. C. Wan, in *Optical Data Storage*, *Proc. SPIE* **1992**, *1663*, 324.

[46] J. J. Cowan, W.D. Slafer, *J. Imaging Sci*. **1987**, *31*, 100.

[47] J. J. Cowan, W.D. Slafer, in *Progress in Holographic Applications, Proc. SPIE* **1986**, *600*, 49.

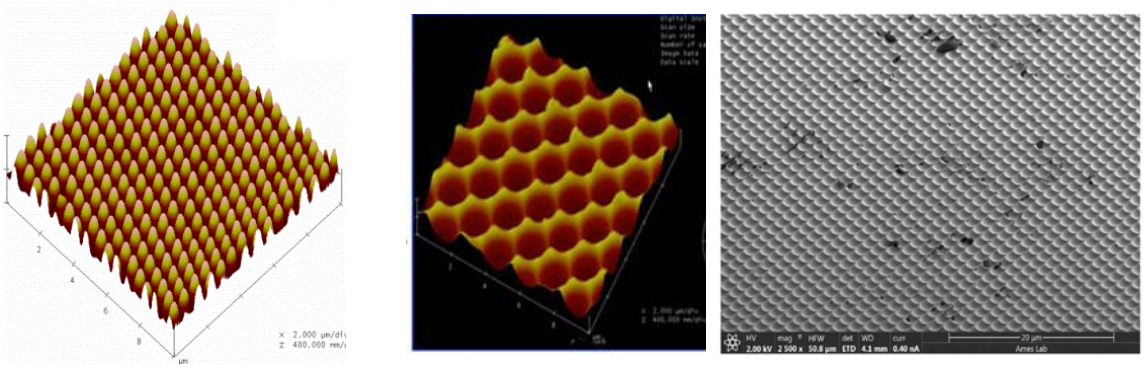

Figure 1. Left: AFM image of a 10x10 μm^2 convex PC with *h* ~320 nm and *a* ~750 nm; Center: AFM image of a 10x10 μm^2 concave PET/CAB with *h* ~250 nm and *a* ~1.75 μm coated with ITO. Right: FIB image (with 20 μm scale bar) of ITO on corrugated PET/CAB showing damaged areas.

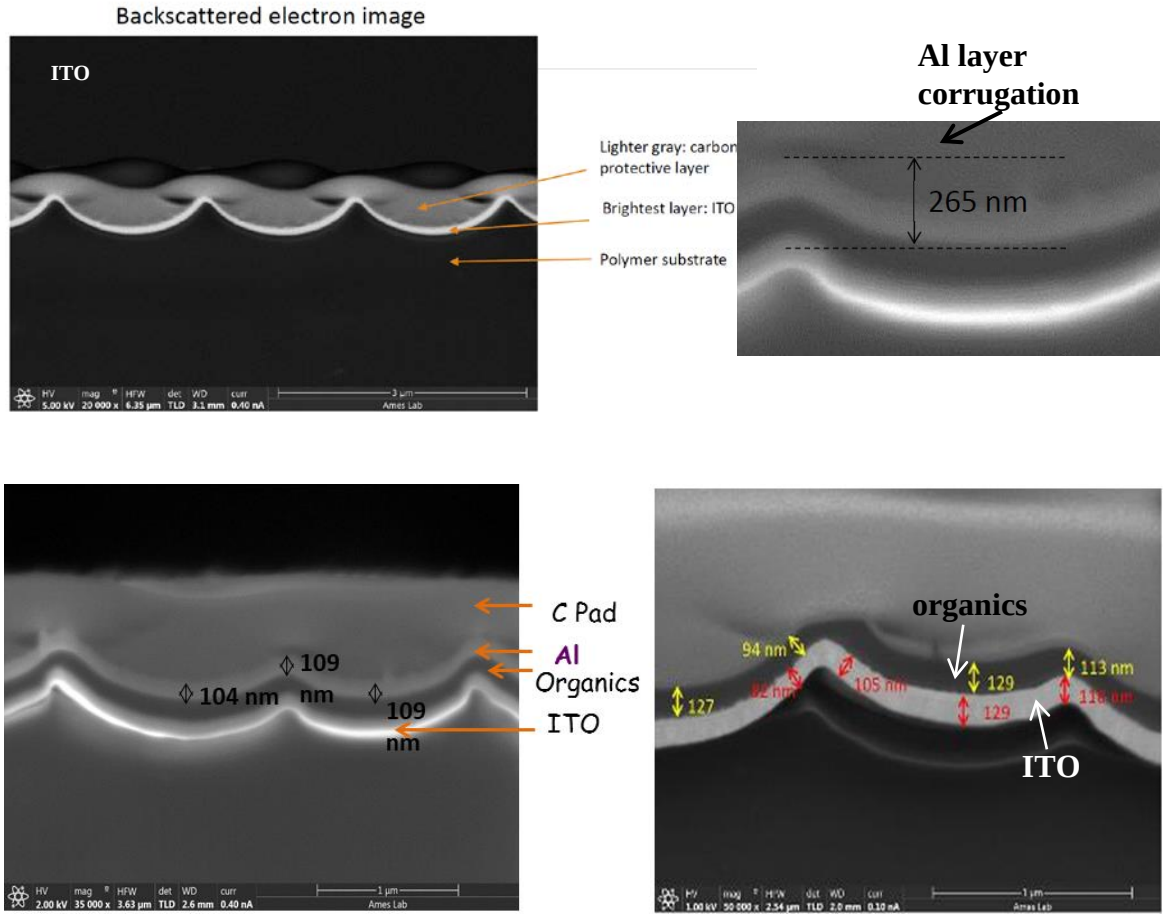

Figure 2. FIB images of patterned ITO and a PhOLED fabricated on PET/CAB with a ~1.75 μm and h ~250 nm. The images show that the OLED structure is largely conformal with the substrate's corrugation (see text).

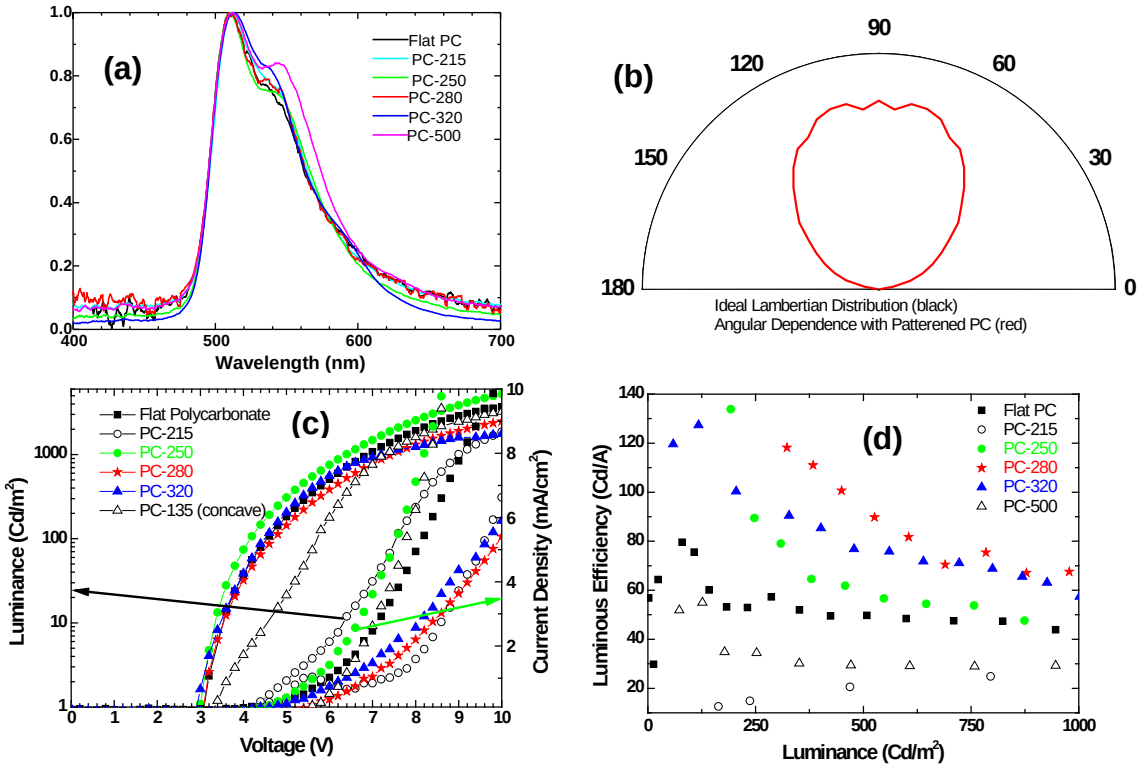

Figure 3. (a) Normalized EL spectra for flat and patterned PC substrates (b) Comparison of the angular distribution of the EL spectrum of an OLED fabricated on patterned PC with ideal Lambertian profile (c) *J-L-V* curves and (d) Luminous efficiency vs brightness of $Ir(ppy)_3$-based PhOLEDs; corrugation heights range from 215 nm (PC-215) to 500 nm (PC-500).

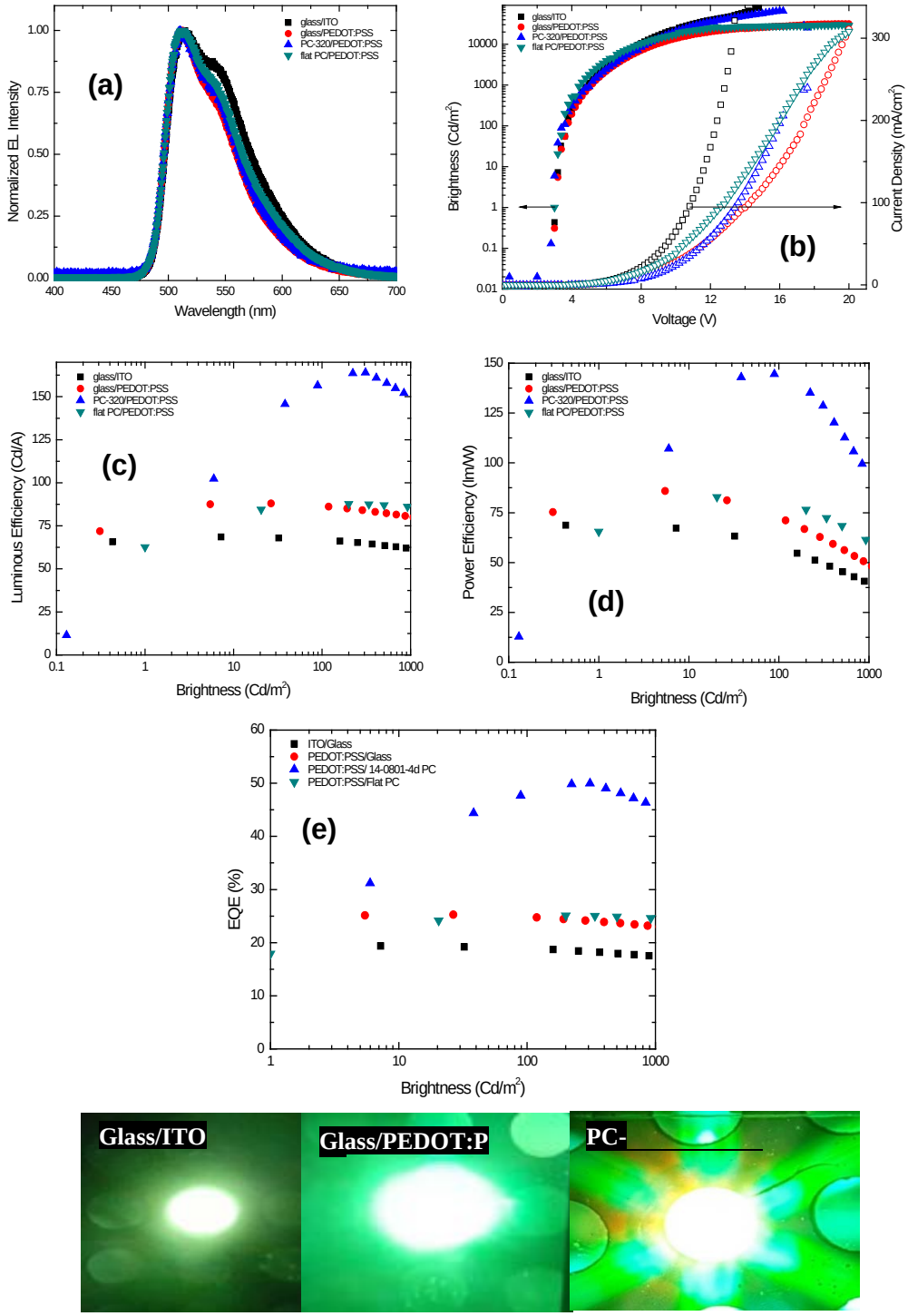

Figure 4. (a) EL spectra, (b) *J-L-V*, (c) Luminous efficiency vs *L*, (d)Power efficiency vs *L*, (e) *EQE-L* for green PhOLEDs on different substrates/anodes, and bottom: images of devices on different substrates/anodes.

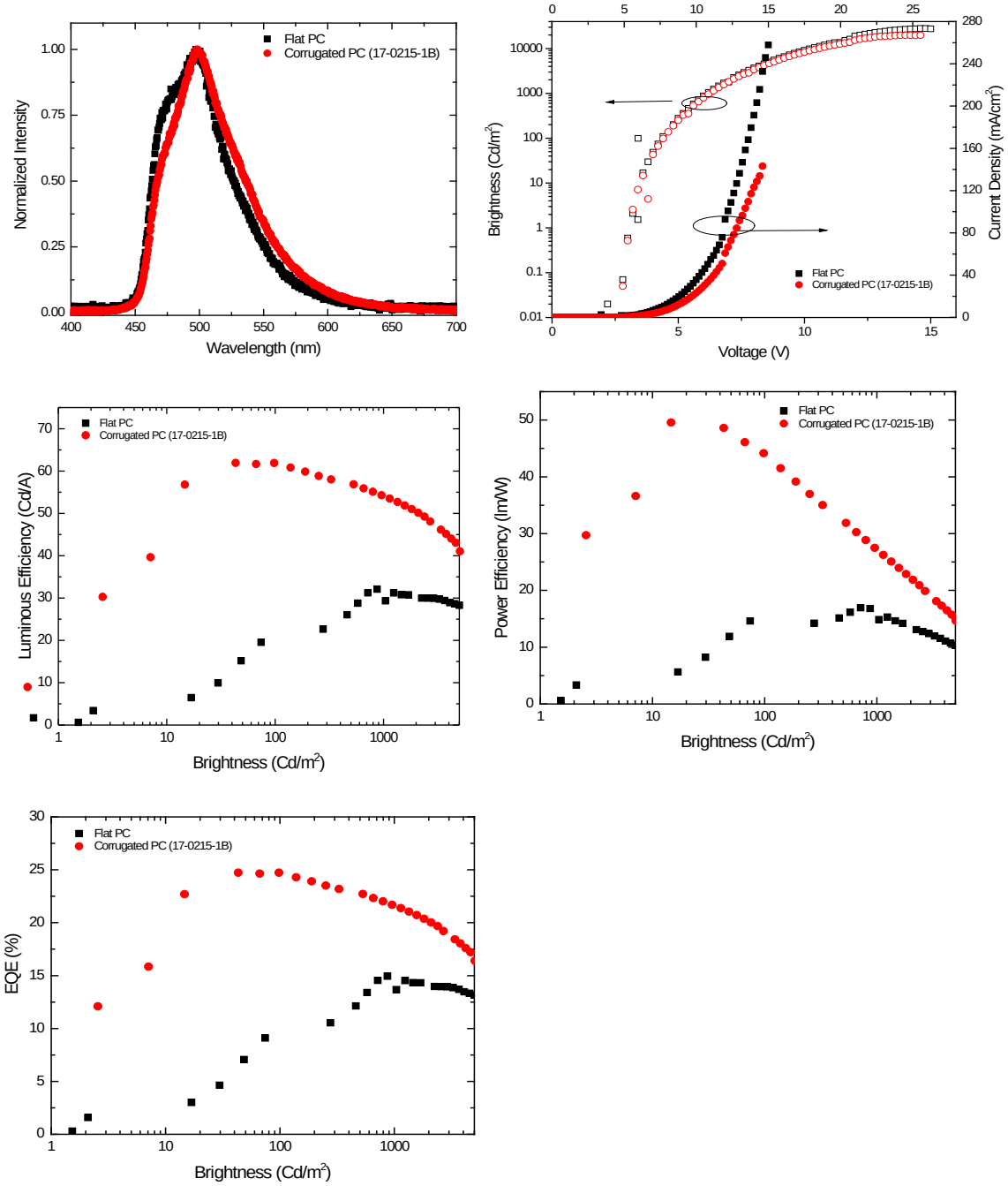

Figure 5. Optoelectronic attributes of blue PhOLEDs fabricated on flat and corrugated PC-280.

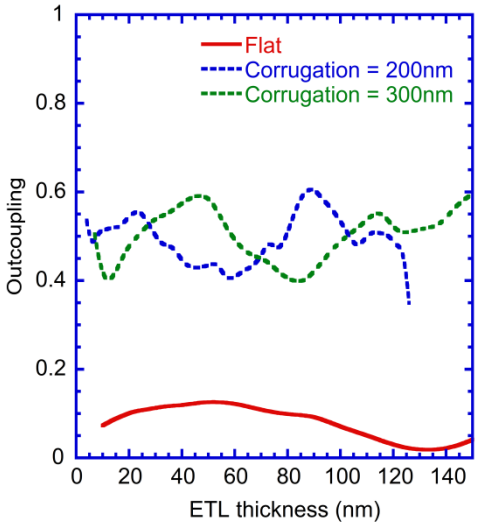

Figure 6. Simulated outcoupling from a green OLED (λ = 510 nm) on a patterned PC/PEDOT:PSS substrate/anode in comparison to a planar glass/ITO OLED using scattering matrix theory. The corrugation heights are 200 and 300 nm.

Table 1. Pattern heights before and after PEDOT:PSS spin coating at various rates.

Substrate	PEDOT:PSS[a)] solution + additive	PEDOT:PSS spin coating speed and duration for each of the two layers	Height measured after coating (nm)
(1) PC-320	6% EG+ 1% Capstone FS35 fluorosurfactant	1000 rpm for 30 s	60
		3000 rpm for 30 s	141-149
		6000 rpm for 30 s	194-203
		6000 rpm for 60 s	208-218
		6000 rpm for 120 s	219-237
		6000 rpm for 30 s Single layer	**~300**
(2) PC-280		6000 rpm for 120 s	166-173
		6000 rpm for 120 s 3 layers	102-112

[a)]The anode consisted of two PEDOT:PSS layers unless otherwise mentioned

Table 2. Green PhOLEDs' peak & 700 Cdm^{-2} efficiencies and the enhancement factor of the PhOLEDs on the patterned substrate.

Substrate/anode	Luminous Efficiency (CdA^{-1})[a)]	Power efficiency (lmW^{-1})[a)]	*EQE* (%)[a)]	Enhancement factors (relative to glass/ITO; glass/PEDOT:PSS; flat PC/PEDOT:PSS)
Glass/ITO	68 (62)	67 (41)	19 (18)	
Glass/PEDOT:PSS	88 (82)	86 (53)	25 (23)	
Flat PC/PEDOT:PSS	88 (86)	82 (64)	25 (25)	
Corrugated PC/PEDOT:PSS	164 @ 300 Cdm^{-2}; (154)	144 @ 100 Cdm^{-2}; (104)	50 @ 300 Cdm^{-2}; (47)	Luminous efficiency: 2.4x; 1.9x; 1.9x Power efficiency: 2.1x; 1.7x; 1.8x *EQE*: 2.6x; 2.0x; 2.0x

[a)]The efficiencies at 700 Cdm^{-2} are in parenthesis.

Table of contents entry:

Strong light extraction from phosphorescent OLEDs fabricated on corrugated polycarbonate with PEDOT:PSS anode is demonstrated. The external quantum efficiency reached 50%, 2.6x that on glass/ITO. (a) 10x10 μm^2 AFM image of a polycarbonate substrate; corrugation height ~320 nm, pitch ~750 nm. (b) Focused ion beam image of OLED fabricated conformally on corrugated plastic. (c) *EQE* vs brightness of green PhOLEDs.

Keyword:
Enhanced light extraction from OLEDs fabricated on patterned plastic substrates

Chamika Hippola, Rajiv Kaudal, Eeshita Manna, Teng Xiao, Akshit Peer, Rana Biswas, W. Dennis Slafer, Tom Trovato, Joseph Shinar,* Ruth Shinar*

Enhanced Light Extraction from OLEDs Fabricated on Patterned Plastic Substrates

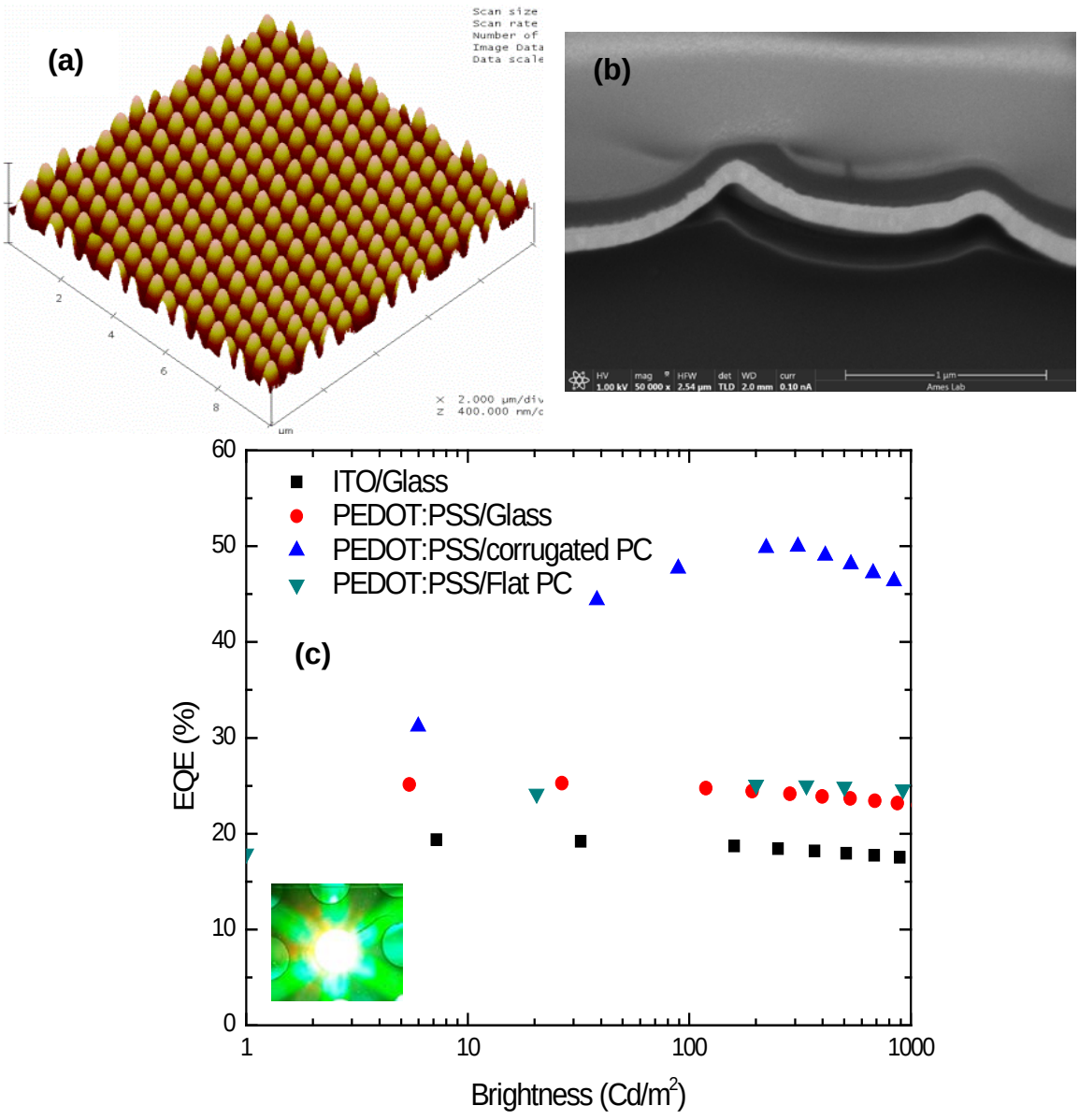

Supporting Information

Enhanced Light Extraction from OLEDs Fabricated on Patterned Plastic Substrates

Chamika Hippola, Rajiv Kaudal, Eeshita Manna, Teng Xiao, Akshit Peer, Rana Biswas, W. Dennis Slafer, Tom Trovato, Joseph Shinar, Ruth Shinar**

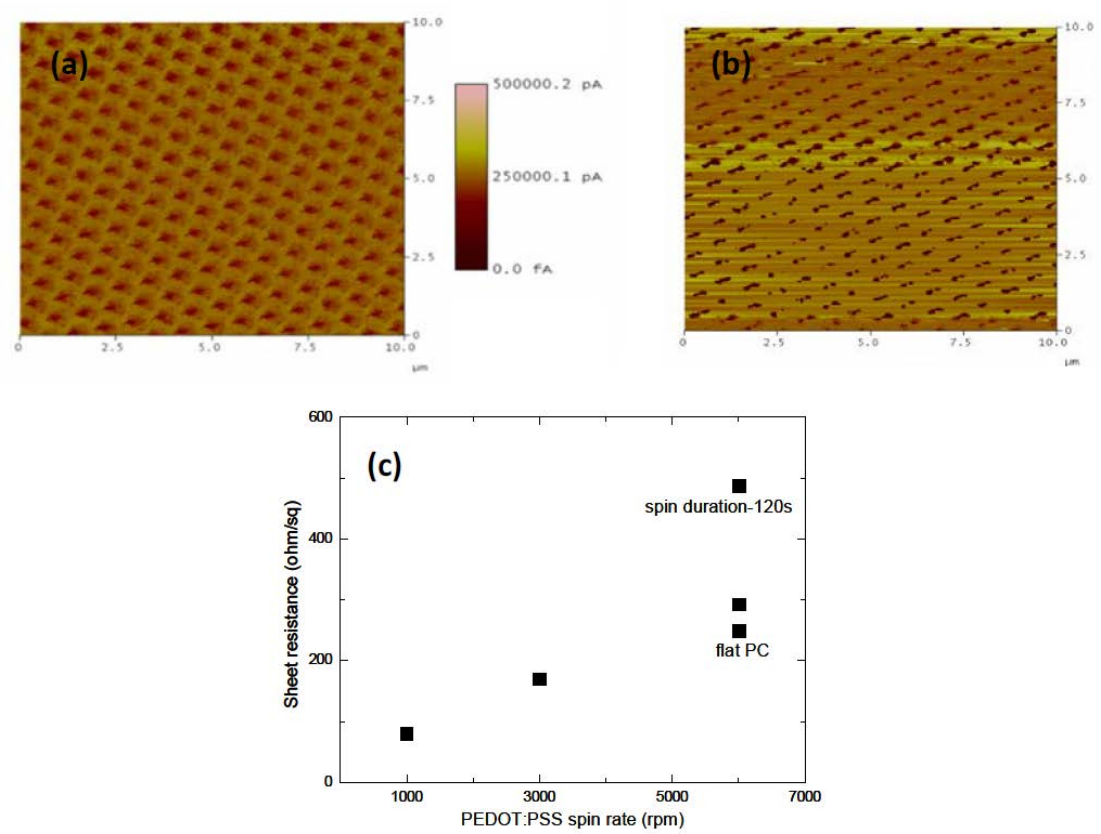

Fig. S1. *Conductivity AFM images of 2–layered PEDOT:PSS spin-coated on patterned PC with h ~320 nm and a ~750 nm for 30 s. (a) 3,000 rpm (~65 nm) and (b) 6,000 rpm (~40 nm). (c) The sheet resistance of two PEDOT:PSS layers coated on flat and patterned PC substrates at different spin coating rates and durations. The spin duration was 30 s unless otherwise noted.*

Table S1. *Corrugation height of the pattern before and after two-layer PEDOT:PSS coating and PhOLED fabrication and the associated enhancement factor*

Sample	Corrugation height			Spin conditions and luminous efficiency enhancement factor
	Before device fabrication (nm)	Following PEDOT:PSS coating (average)	After device fabrication (nm)	
PC-320	320	~200		6000 rpm/30 s
PC-320	320	~215		6000 rpm/60 s
PC-320	320	~230		6000 rpm/120 s
PC-320 green	320		135-170	~1.6x
PC-135 blue	135 (inverted)		118	~1.5x
PC-320 blue	320		190	~3.0x

Table S2. *Comparison of attributes of green and blue PhOLEDs fabricated on different substrates with two layers of PEDOT:PSS (total thickness ~ 65 nm) as the anode.*

	Sample	Turn on voltage (V)	Max. luminous efficiency (CdA^{-1})	Corresponding EL (Cdm^{-2})	Luminous Efficiency @ 1000 Cdm^{-2}
Green	Flat PC	3.0	80	79	44
$Ir(ppy)_3$-based	PC-215	4.0	28	1321	27
	PC-250	3.0	89	247	47
PhOLEDs	PC-280	3.0	118	323	64
	PC-320	3.0	127	118	57
	PC-500	3.4	54	127	29
Blue	Flat PC	3.3	29.2	110	9.6
FIrpic-based	PC-320		87	140	17.9
	PC-135		45.2	408	30.9
PhOLEDs					

The structure of the green PhOLEDs (Design 1) was:

PEDOT:PSS (2 layers) anode / MoO_3 (1 nm) / 10% MoO_3:NPB (22.5 nm) / NPB (22.5 nm)/ 6% $Ir(ppy)_3$:CBP (11 nm) / BPhen (40 nm) / LiF (1nm) / Al (100 nm);

and that of the blue devices (Design 1) was

PEDOT:PSS (2 layers) anode / MoO_3 (5 nm) / (TAPC) (30 nm) / 2% FIrpic: mCP (20 nm) / 3TPYMB (10 nm) / BPhen (40 nm) / LiF (1 nm) / Al (100 nm)

Finite difference time domain (FDTD) simulations

An alternative simulation approach to the scattering matrix that provides additional physical insights is the FDTD simulation using the Lumerical package. That package has the ability to handle complex OLED corrugations, in a real space approach where the OLED is discretized in a real space grid (**Figure S2**). The emissive layer conforms to the contour of the corrugated substrate. The random orientation of the dipoles is modeled by a superposition of classical dipoles that are oriented in the three Cartesian directions (*x, y*, and *z*, with the *z* direction perpendicular to the substrate). The dipoles can reside at varying distances from the PC/air interface. That is, the two extremal positions of the dipole correspond to (i) the 'highest' position, farthest from the PC/air interface, where the dipoles form a ring-like distribution above the corrugation peak, and (ii) the 'lowest' position, where the dipoles are located above the troughs of the anode corrugation, closest to the substrate/air interface. The distribution of emitted power was monitored (i) inside the OLED emissive layer (P_{in}) and (ii) in the air region outside the substrate (P_{out}), with the ratio P_{out}/P_{in} providing the outcoupling factor. Based on the FDTD simulations performed with corrugated OLEDs of varying pitch *a* we infer that 750 nm is optimal for blue OLEDs and benefits green OLEDs, whereas 500 nm is slightly better for red OLEDs. Thus a single pitch around 750 nm may be a near-optimal choice for white OLEDs. The FDTD simulations indicated that the largest enhancements were obtained for a range of pitch values ca 500-750 nm. Accordingly we simulated the

enhancement of light for the two extremal positions of the dipoles as a function of the wavelength of the emission and averaging over the three dipole orientations. As an example, for a green OLED an enhancement factor of ~1.6x was obtained for h = 200 nm and a = 500 nm for an OLED with 180 nm anode + HTL (90 nm each, glass/ITO OLED) and 70 nm ETL. The dipoles farther from the PC/air interface offer larger enhancement (~1.6x), than those residing closer to the substrate. Further exploration of dipole positions, pitch values, and corrugation heights are necessary to further optimize the enhancements. The effect on the maximal η_{out}, of changing h from 200 to 300 nm is small as indicated by the scattering matrix simulations.

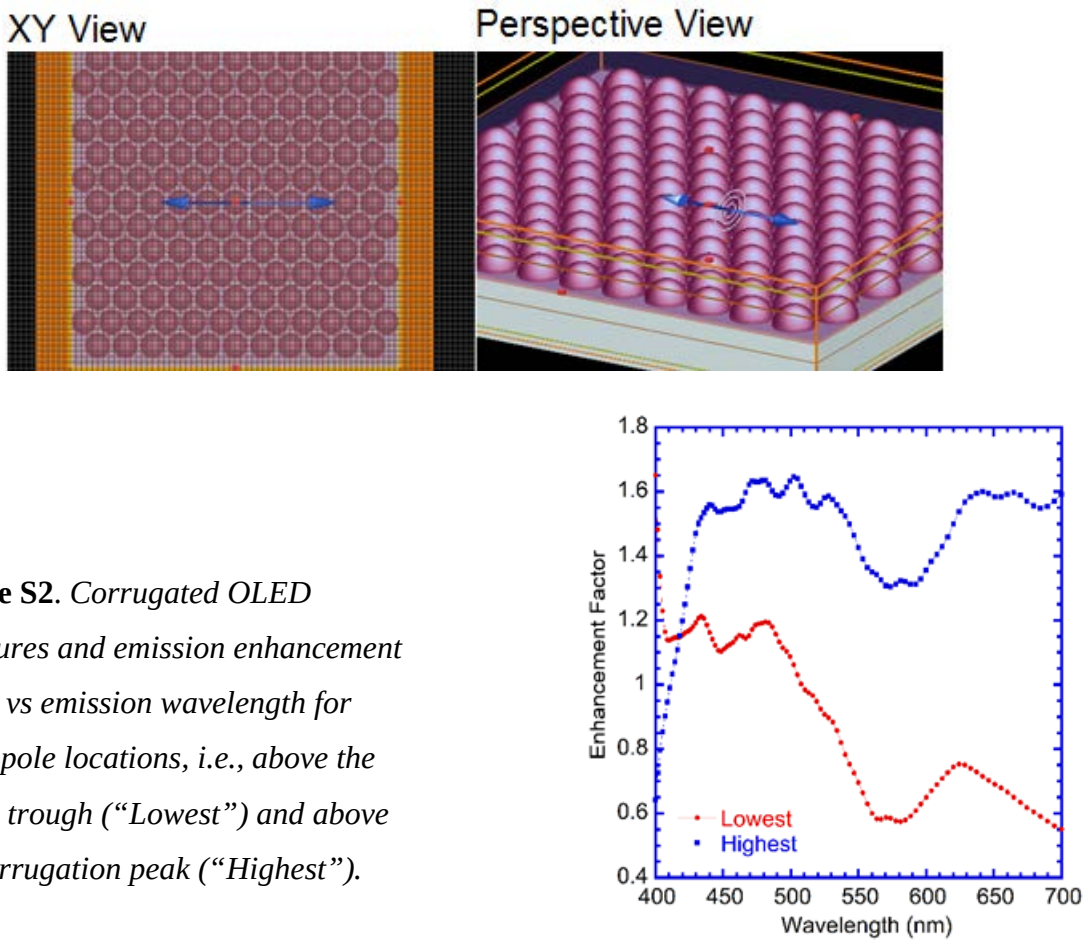

Figure S2. *Corrugated OLED structures and emission enhancement factor vs emission wavelength for two dipole locations, i.e., above the anode trough ("Lowest") and above the corrugation peak ("Highest").*